

OPTIMAL DESIGN OF GAS ADSORPTION REFRIGERATORS

FOR CRYOGENIC COOLING*

C. K. Chan
Jet Propulsion Laboratory
4800 Oak Grove Drive
Pasadena, CA 91109

ABSTRACT

The design of gas adsorption refrigerators used for cryogenic cooling in the temperature range of 4K to 120K has been examined. The functional relationships among the power requirement for the refrigerator, the system mass, the cycle time and the operating conditions were derived. It was found that the precool temperature, the temperature dependent heat capacities and thermal conductivities, and pressure and temperature variations in the compressors had important impacts on the cooling performance. Optimal designs based on a minimum power criterion were performed for four different gas adsorption refrigerators and a multi-stage system. The estimates of the power required and the system mass were within manageable limits in various spacecraft environments.

NOMENCLATURE

a	constant
b	Van der Waal's volume
c	constant
C	specific adsorptance, mass ratio of gas adsorbed to adsorbent
C_p	heat capacity
D	container diameter
h	enthalpy
k_g	gas conductance
m	mass
\dot{m}	mass flowrate
M	molecular weight
P	pressure
\dot{Q}	heat transfer rate
Q	heat
R	universal gas constant
t	time
T	temperature

* This paper represents one phase of research carried out at the Jet Propulsion Laboratory, California Institute of Technology, under NASA Contract NAS7-918.

ΔU heat of adsorption
 V volume
 x adsorption potential
 x_m mass ratio of container to adsorbent
 α correlating parameter
 β parachor
 γ correlating parameter
 σ_y yield strength
 ρ density
 Δ difference
 δ gas gap

SUBSCRIPTS

$1, 2, 3, 4$ compressor states illustrated in Fig. 2
 a, b, c, d, e, f thermodynamical states of gas illustrated in Fig. 3
 cr critical
 C heat sink, or cooling
 H high, or heating
 L low
 \bar{p} precool
 r refrigeration chamber
 s container
 α adsorbent

INTRODUCTION

The potential use of gas adsorption compressors as a gas source for cryogenic refrigerators has become fairly promising for sensor cooling, because of their inherent merit of no moving parts and the fact that a low temperature heat source [1] can act as the power source. Conceptually, a Joule-Thomson (J-T) cooling device [2] can be coupled to a set of gas adsorption compressors which operate cyclically between desorption and adsorption modes. These compressors liberate and compress the gas during the desorption mode and re-adsorb the gas during the adsorption mode. A system design utilizing J-T cooling and two adsorbent compressors was proposed by Chan [1] while a multi-stage system to handle various refrigeration temperature requirements was proposed by Chan, Tward and Elleman [3].

This paper presents a generalized methodology to design such gas adsorption refrigeration systems and to evaluate their performance. In designing the J-T valve and heat exchanger, gas flow and other thermodynamical conditions such as pressures and temperatures will be determined for a given cooling load at a given refrigeration temperature. The gas adsorption compressor design will include the adsorbent mass, the temperature variation, the container volume, the cycle time and the power requirement. Optimization analyses will be emphasized for the power and the mass criteria. These analyses will provide information about the optimal operating conditions for various gas adsorption refrigerators.

GAS ADSORPTION REFRIGERATION SYSTEMS

The gas adsorption refrigeration system using a J-T valve and heat exchanger and two gas adsorption compressors is shown in Fig. 1, while the thermodynamical paths for the compressor and the J-T valve for an idealized system are shown in Figs. 2 and 3, respectively.

Starting from the state point 1 in Fig. 2, the adsorbent is at its lowest temperature T_1 , the lowest pressure P_1 but highest adsorptance C_1 when the adsorbent chamber A in Fig. 1 is heated with no gas outflow (process 1-2 in Fig. 2). Both the temperature and the pressure inside the chamber would increase with little change of adsorptance concentration for an ideal compressor. At point 2 in Fig. 2 the pressure is high enough to push open the check valves 1 and 4 and close valves 2 and 3 in Fig. 1. The gas outflow causes the adsorptance to drop coupled with further temperature increase. In the ideal situation, the gas flows at a constant pressure as represented by the process 2-3 in Fig. 2.

When Chamber A is at the state point 1, chamber B will be at the state point 3, so when A is heated, heat is removed from chamber B. This will cause the temperature in B to drop and gas can be adsorbed as indicated by processes 3-4 and 4-1 in Fig. 2.

If the compression action of chamber A and the suction action of chamber B could be synchronized, then the high-pressure gas would flow through the precooler and the counterflow heat exchanger where it is cooled to a lower temperature before it expands through a J-T valve. Upon expansion, the gas enters the refrigeration chamber in the form of a two-phase mist. The thermodynamical states of the gas before the precooler, the counter-flow heat exchanger and the J-T valve are represented by state points a, b, and c, respectively, in Fig. 3. The throttling process moves the state point from c to d along a constant enthalpy process. The refrigeration load causes the vaporization of the liquid. Hence, the outlet of the refrigeration chamber is at state point 3 in Fig. 3. Upon the return passage through the counter-flow heat exchanger, the outlet temperature of the gas at state point f is the same as the inlet temperature (state point b). The low pressure in the refrigeration chamber is maintained by the suction process in chamber B where the gas is being adsorbed.

At the state point 3, when the gas inventory in chamber A has been depleted, the heat flow of both chambers reverses direction. Chamber B now functions in the role of the compressor while chamber A functions as the suction pump. The state point of compressor A moves from 3 to 4 and then back to 1. Thus, the compressor completes its cycle by heating and then cooling. For the two-compressor system described here, there are two periods during the cycle when there is no gas flow (processes 1-2 and 3-4). This problem can be alleviated by combining this system with another similar set of two compressors which operates at ninety degrees out of the phase of the

first two, or by the use of ballast tanks so that continuous gas flow can be maintained at the J-T expander.

J-T COOLING

Considering the J-T expansion system with the precooler as shown in Fig. 1, the thermodynamic states of the gas downstream of the compressor are represented on the T-S diagram shown in Fig. 3. The state point of the gas after exiting the precooler is represented by the point b in Fig. 3.

The gas is further cooled to the state point c after it passes through the counterflow heat exchanger. The throttling of the high-pressure gas to the low-pressure region is represented by the path c-d. In the refrigeration chamber the refrigeration load causes the liquid to vaporize as shown by the path d-e. While passing through the counter flow heat exchanger, the gas is heated from point e to point f. From the total energy balance, the refrigeration load \dot{Q}_R is related to the mass flow as:

$$\dot{Q}_R = \dot{m}(h_f - h_b) \quad (1)$$

where \dot{m} is the mass flow rate through the J-T valve, h_f is the enthalpy of the outlet gas at the low-pressure side of the counterflow heat exchanger and h_b is the enthalpy of the inlet gas after the precooler. For a given refrigeration temperature T_R , the temperature at state point d must equal to T_R . This determines the low-pressure isobar at d, e and f because there is only one relationship between saturation pressure and saturation temperature.

From a designer's point of view there are two adjustable parameters: (1) the gas temperature, T_b after the precooler and (2) the pressure, P_c upstream of the J-T valve. As the pressure decreases and as T_b increases the required mass flow increases as shown in Fig. 4. The mass flow rate corresponds directly to the adsorbent mass in the compressor. However, a high-pressure condition would add structural mass to the system. As well, the maximum usable pressure is restricted by the isotherms and the thermal cycle of the compressor. The precooling temperature is restricted by the availability of the heat sink.

GAS ADSORPTION COMPRESSOR DESIGN

In the refrigeration cycle, a compressor provides the required gas flow at the desired pressure and temperature. Since the mass flow is related to the pressures of the gas from the compressors based on the refrigeration requirement as shown by equation (1), the parameters for the gas adsorption compressor such as the adsorbent mass, the container mass, the energy

required to power the compression, and the temperature swing of the adsorbent for the compression and decompression cycle, are expected to relate to the mass flow, the heat source, temperatures T_H and the heat sink temperature, T_C . If a gas heat switch [4] is used to control the heat into and out of the compressor, then the cycle time for the adsorption cycle may be controlled by the performance of the switch.

ISOTHERMS

The gas-adsorption compressor depends on the adsorption characteristics of the gas by the adsorbents at different temperatures. When the gas is brought into contact with the adsorbent, some of the molecules striking the solid surface will be retained for a finite period of time, resulting in a significantly higher molecular concentration at the surface than in the gas phase. The forces holding the molecules to the solid are due to molecular interactions. This process is known as physical adsorption and has been studied, both at ambient and cryogenic temperatures. A comprehensive review of the subject at cryogenic temperatures can be found in Reference [5]. However, much of the past experimental data for adsorption of various cryogenic gases by such adsorbents as charcoal, zeolite and silica gel are available only in the low pressure range. This is due to the fact that the main application of gas adsorption has been related to either low-pressure gas removal or to cryopumping. Gas adsorption at the higher pressures which are needed for a workable gas adsorption compressor, has only recently become available [6, 7].

For the design of an adsorption compressor, it would be convenient to express analytically the adsorption of the gas on the adsorbent as a function of pressure and temperature. For this reason, the isotherm data for hydrogen and neon, nitrogen and helium gases have been correlated with a similarity parameter, the adsorption potential x , given by

$$x = \frac{RT}{\beta} \ln \left(\frac{P_{cr}}{P} \left(\frac{T}{T_{cr}} \right)^2 \right), \quad (2)$$

where β is the parachor, R is the universal gas constant, T is the adsorbent temperature, P is the gas pressure, T_{cr} is the critical temperature of the gas and P_{cr} is the critical pressure of the gas.

The data were fitted to an expression of the form

$$C = \frac{M}{b} \alpha e^{-\gamma x} \quad (3)$$

where the specific adsorptance C is the gas mass adsorbed per unit mass of

charcoal, M is the gas molecular weight, b is the Van der Waal's volume, and α and γ are correlating parameters determined from the data.

POWER REQUIREMENT

The power requirement for the refrigeration cycle is best represented by the specific power which is defined as the ratio of the heat input for the cycle to the refrigeration load.

During the compression period, the total refrigeration load is

$$Q_r = m_\alpha \Delta C (h_f - h_b) \quad (4)$$

where m_α is the adsorbent mass and $m_\alpha \Delta C$ represents the gas mass liberated during the compression. The heat required for gas liberation is given by

$$Q_H = (m_\alpha C_{p\alpha} + m_s C_{ps}) \Delta T + m_\alpha \Delta C \Delta U \quad (5)$$

where m_α and m_s are the masses of the adsorbent and the container, respectively, $C_{p\alpha}$ and C_{ps} are the heat capacities of the adsorbent and container and ΔT is the maximum temperature swing of the adsorbent and ΔU is the isosteric heat of adsorption which satisfies an equation similar to the Clausius-Clapeyron equation, i.e.,

$$\Delta U = -R \left(\frac{\partial \ln P}{\partial \left(\frac{1}{T} \right)} \right) C \quad (6)$$

In equation (5), the heat capacity of heat enhancement elements inside the adsorbent bed can be lumped into the $m_s C_{ps}$ term. Combining equations (4) and (5), the specific power of the refrigerator is given by

$$\frac{Q_H}{Q_r} = \frac{(C_{p\alpha} + x_m C_{ps}) \Delta T}{(h_f - h_b) \Delta C} + \frac{\Delta U}{(h_f - h_b)} \quad (7)$$

where x_m is the ratio of container mass to adsorbent mass.

Since h_f and h_b are functions of the high pressure P_H and the low pressure P_L , as well as the precooler temperature T_D , the specific power is a function of P_H , P_L , T_1 , T_p , ΔT , and ΔC , but independent of the cycle time.

CONTAINER MASS

In estimating the container mass ratio in Eq. (6), a cylindrical container completely filled with the adsorbent is assumed for this model. By imposing the restriction that the Hooke stress of the cylindrical wall resulting from internal pressurization is limited by the yield strength of the container material, the mass of the container to the adsorbent mass can be expressed as [1]

$$x_m = \frac{m_s}{m_a} = \frac{2\rho_s P_H}{\rho_a \sigma_y} \quad (8)$$

where ρ_s is the density of container material, ρ_a is the density of the adsorbent, P_H is the maximum gas pressure in the compressor and σ_y is the yield strength of the material.

CYCLE TIME

Assuming a gas heat switch similar to the one mentioned in ref. [4] is used to conduct the heat out of the cylindrical compressor through a gas gap to the heat sink at temperature T_C , the time required to cool the compressor from T_3 to T_1 is given by

$$t_C = \frac{\rho_a \bar{C}_p \delta D}{4k_g} \ln \left(\frac{T_3 - T_C}{T_1 - T_C} \right) \quad (9)$$

where

ρ_a = adsorbent density

$$\bar{C}_p = (C_{pa} + x_m C_{ps}) \quad (10)$$

δ = gas gap

k_g = gas conductance

and D = diameter of the compressor cylinder.

The gas conductance k_g can usually be expressed as

$$k_g = \left(\frac{T}{a} \right)^c \quad (11)$$

where a and c are correlation constants (Table 1).

In our experience the cycle time of the heatup and the cooldown of the complete cycle is usually limited by the cooling period t_C . Hence, if the

cooling time equals the heating time because of the synchronization requirement, then the cycle time t_o is given by

$$t_o = 2t_c = \frac{\rho_\alpha \bar{C}_p \delta D}{2k_g} \ln \left(\frac{\Delta T}{T_1 - T_C} + 1 \right) \quad (12)$$

When the adsorbent is heated at constant pressure (process 2-3 in Fig.2) the mass flow required for refrigeration comes from the liberation of the adsorbed gas. By assuming a uniform gas flow over the heating period, the mass flow rate \dot{m} is related to the adsorbent m_α and the cooling period t_c by

$$\frac{\dot{m}}{m_\alpha} = \frac{\Delta C}{t_c} \quad (13)$$

By substituting equations (9) and (1) into equation (13), then the adsorbent mass for a unit of refrigeration load can be expressed as:

$$\frac{m_\alpha}{\dot{Q}_r} \left(\frac{4k_g}{\rho_\alpha \bar{C}_p \delta D} \right) = \frac{\ln \left(\frac{\Delta T}{T_1 - T_C} + 1 \right)}{(h_f - h_b) \Delta C} \quad (14)$$

The total mass of the compressor is then

$$m = m_\alpha (1 + x_m) \quad (15)$$

Hence, the compressor mass, unlike the specific power, is a function of the cycle time which depends on the physical properties of the heat switch as well as the temperature swing of the cycle (ΔT) and the temperature difference between the heat sink and the minimum of the compressor cycle.

DATA

Four different refrigeration systems using charcoal as the adsorbent, have been studied. The adsorbed gases are nitrogen, helium, hydrogen and neon. The physical properties of these gases are shown in Table 1 which also includes the constants for the gas conductivity correlations of hydrogen and helium (eq. 11) and the constants for the isotherms (eq. 3).

Adsorption isotherms of hydrogen and neon on charcoal have been obtained in the pressure range from 1 to 100 atmospheres and in the temperature range from 77 to 200K [7]. These high pressure data compare well with the Kidney and Hiza data [8] in the medium temperature and pressure ranges. Adsorption

of nitrogen in the high pressure range was obtained by Yang et al [6], Cook [9], and Tward [10]. The adsorptance from Yang's and Tward's data is about two times those found by Cook and Kidnay and Hiza. The correlating coefficients of the generalized equation (2) for the Kidnay and Hiza's as well as Tward et al isotherms, are presented in Table 1. The density, the temperature dependent heat capacities and the average heat capacities over a certain temperature range for charcoal, stainless steel and copper as well as the temperature dependent yield strength of stainless steel are presented in Table 2. It was found that the temperature dependent heat capacities can be expressed as

$$C_p = \left(\frac{T}{a}\right)^c \quad (16)$$

where C_p is the heat capacity in cal/g-K, T is the temperature in K, a and c are correlation constants which have the following values for charcoal; $a = 775.57$, $c = 1.69877$, for $20K < T < 500K$. For stainless steel, $a = 344.89$, $c = 2.0401$, for $20K < T < 110K$, whereas $C_p = 0.1$ cal/g-K for $T > 110K$.

OPTIMAL DESIGN

The mass flow rate, given by equation (1), provides the simplest way to have some insight into the optimal operating pressure conditions.

The mass flow rates per unit cooling power as a function of the compressor high pressure for four different gases is shown in Fig. 4. The low pressure for all these four cases is 1 atm while the precool temperatures for helium, hydrogen, neon, and nitrogen are 20K, 77K, 77K and 150K, respectively. Plots such as these which consider only the J-T cooler can be used to determine the minimum flowrate required.

It is always desirable to have a gas adsorption refrigerator that weighs the least, occupies the least space and requires the least power to operate. Specific power given by equation (7), is a good indication of the power required. For a given adsorbent material and container material,

$$\text{Specific Power} = f(P_H, P_L, T_1, T_3, T_p) \quad (17)$$

The mass of the compressor given by equations (14) and (15), is a function of the heat switch design parameters (δ , D , and k_g) in addition to the temperature and the pressure parameters:

$$\frac{\dot{m}}{\dot{Q}_r} = f \left(P_H, P_L, T_1, T_p, T_C, \frac{k}{\delta D} \right) \quad (18)$$

Among the six temperature and pressure parameters, the refrigerator chamber pressure P_L is determined by the refrigeration temperature T_r and the pre-cool temperature T_p is determined by the availability of the heat sink (temperature T_C). The lowest temperature in the compressor cycle T_1 has to be higher than T_C . However, for a given P_L , higher adsorptance is obtained by having T_1 as low as possible. Hence, T_1 should be greater than but close to T_C .

In the present parametric study, the specific power and the compressor mass are determined for various values of P_H , P_L , T_1 , T_3 , T_p for helium, hydrogen, neon and nitrogen systems. In the calculation, the counter flow heat exchanger is assumed to be perfect, i.e., the inlet gas temperature is equal to the outlet gas temperature, the precool temperature and the sink temperature are equal and the difference between the temperature T_1 and the heat sink temperature T_C is 1°K . The temperature dependent effects of the heat capacities (eq. 16) and the gas conductance (eq. 11) are incorporated into the calculations.

A computer program was written to perform the calculations. The outputs of the computer program include the specific power, the compressor mass and the mass flowrate for a unit of refrigeration load, the cycle time, the change of adsorptance, the container/adsorbent mass ratio, the heat capacities of the adsorbent and the container. In the compressor mass and the cycle time calculations, a gas gap of 0.01 cm and a compressor cylinder of 1 cm are used. It would be simple to calculate these two parameters for other heat switch dimensions because of the linear relationship between these parameters and those dimensions as illustrated by equations (9) and (14).

The results of a typical numerical calculation are illustrated in Fig. 5. It can be generally concluded that, for a given precooling temperature, a given low compressor pressure level and temperature, there exists a minimum specific power. For most efficient operation, one would like to operate the system at the pressure and temperature values corresponding to the minimum specific power. For example, the specific power for the helium system has a minimum value of 6.5 at $P_H = 20$ atm and $T_H = 51\text{K}$ for $T_p = 20\text{K}$, $T_C = 20\text{K}$, $T_1 = 21$ and $P_L = 1$ atm. The minimum specific power decreases as the low pressure level increases and decreases with the precool temperature. The minimum power for the four systems and the corresponding compressor masses for unit refrigeration load, cycle time, and operating conditions are tabulated in Table 3. The compressor mass corresponding to the minimum power is not necessarily the minimum value in the parametric study. Thus, the optimal point based on minimum power is not necessarily the optimal point based on minimum mass.

MULTISTAGE DESIGN

A schematic diagram of a multistage refrigerator proposed by Chan, Tward and Elleman [3] is shown in Fig. 6. To illustrate the application of the optimal design method to the design of this multistage system, consider a helium refrigerator of 1 mW cooling at 4.2K. J-T output pressure must be at 1 atm corresponding to the vapor pressure of helium at 4.2K. For minimum Specific Power (S.P.) the high pressure should be 20 atm. If a hydrogen stage refrigerator can provide a heat sink of 20K for precooling the gas and cooling the helium compressor, then the maximum temperature in the helium compressor is 51K. Under these thermodynamic conditions, the S.P. for the helium compressor is 6.5 (Table 3). In other words, the total heat dumped into the hydrogen stage is 7.5 mW (i.e., 6.5 mW + 1 mW).

If a similar procedure is followed in designing the hydrogen stage, for a minimum S.P. of 66.6, the adsorption compression should be operated between 1 atm and 40 atm, for a temperature swing of the compressor between 78K and 218K with the gas precooling temperature at 77K. Hence, the heat dumped to the 77K heat sink is $(66.6 \times 7.5 + 7.5)$ or 507 mW.

The 77K heat sink is provided by the nitrogen stage. The S.P. for that stage is 54.2 for $P_L = 1$ atm, $P_H = 60$ atm, $T_1 = 134$ K, $T_3 = 474$ K and $T_p = 133$ K. The 150K heat sink for the nitrogen stage can be provided by a passive radiator at 133K. The total heat load on the radiator will be 28W.

The total heat load on the radiator could be reduced if we adopted the following heat recovery schemes at each stage. Half of the heat for the heat-up process of the He compressor can be obtained from the cool-down process of the He compressor of the same stage. Hence, the total heat dumped onto the hydrogen stage will be $(6.5/2 + 1)$ or 4.25 mW. This scheme is defined here as internal heat recovery. The other half of the heat to heat up the He compressor can be obtained from the cool-down phase of the upper stage compressor. This scheme is defined here as external heat recovery.

If a similar heat recovery procedure is followed in designing the hydrogen stage, for minimum power of 66.6, the adsorption compression should be operated between 1 atm and 40 atm, for a temperature swing of the compressor between 78K and 218K with the gas precooling temperature at 77K. Hence, the heat dumped to the 77K heat sink is $(66.6 \times \frac{4.25}{2} + 4.25)$ or 146 mW.

As before, the 77K heat sink is provided by the nitrogen stage, where the specific power is 54.2 for $P_L = 1$ atm, $P_H = 60$ atm, $T_1 = 134$ K, $T_3 = 474$ K and $T_p = 133$ K. The heat sink for the nitrogen stage can be provided by a passive radiator at 133K. The total heat load on the radiator will be 4.1 W.

As shown in Fig. 7, the use of the internal heat recovery scheme reduces the heat load onto the radiator by a factor of 7. The use of the external

heat recovery scheme does not seem to greatly improve the efficiency of the overall system. Effects of additional control systems needed for the heat recovery to the multistage system design, remain to be examined.

The compressor mass calculated in the optimal design is based on a gas gap of 0.01 cm and the cylinder diameter of 1.0 cm. Suppose the gas gap is 0.1 cm instead of 0.01 cm, the mass and the cycle time will be simply 10 times those values tabulated in Table 3. If these 10 times conservative values were used to compute the two compressors for each system, then the compressor mass, the cycle time and the power for each stage are shown in Table 4. This corresponds well with some of the experimental results [11]. The mass of the J-T valve and the heat exchanger ($m_{J-T} + m_{H.E.}$) is estimated from the present miniature J-T technology; 14 gm per 40 cc (S.T.P.)/sec. gas flow [2].

Hence

$$m_{J-T} + m_{H.E.} = \frac{(14 \text{ gm})\dot{m}}{(40) M} \quad (22400) \quad (19)$$

where \dot{m} is the mass flow rate (gm-s/W)

M is the molecular weight.

The mass of each (m_{sy}) system consisting of two compressors, the J-T valve and the heat exchanger is $2m + m_{J.T.} + m_{H.E.}$. The total power required by the three stages without heat recovery will be

$$\dot{Q}_r \left\{ \begin{aligned} & \left[(S.P.)_{He} + 1 \right] + \left[(S.P.)_{He} + 1 \right] \left[(S.P.)_{H_2} + 1 \right] \\ & + \left[(S.P.)_{He} + 1 \right] \left[(S.P.)_{H_2} + 1 \right] \left[(S.P.)_{N_2} + 1 \right] \end{aligned} \right\} \quad (20)$$

and total mass of the three stages is

$$\dot{Q}_r \left\{ \begin{aligned} & (m_{sy})_{He} + \left[(S.P.)_{He} + 1 \right] (m_{sy})_{H_2} \\ & + \left[(S.P.)_{He} + 1 \right] \left[(S.P.)_{H_2} + 1 \right] (m_{sy})_{N_2} \end{aligned} \right\} \quad (21)$$

For the case without heat recovery, the total heat rejected onto the radiator is 28.5 W and the total mass without the radiator is 1 Kg. However, with the internal heat recovery and the external heat recovery schemes, the heat rejected and the total mass are reduced by a factor of 7. Effects of heat recovery schemes on the multi-stage design are illustrated in Fig.7.

CONCLUSIONS

The design of gas adsorption refrigerators has been examined from the aspect of the minimum power criterion which is an important aspect, but it should not be the only one. The weight, versatility, and the interaction of the system with other spacecraft components should be considered in the merit evaluations of the design. The methodology and the functional relationships derived here, would provide the fundamental base for such merit evaluations. The weight and the power estimated for the multi-stage system seem to be manageable in spacecraft environments. From these design analyses, it is observed that gas adsorption systems could perform cooling below the 90K temperature range where radiators are ineffective, perform longer term cooling than stored cryogenes, and offer better reliability and vibration-free operation in comparison to mechanical refrigerators.

ACKNOWLEDGEMENT

This paper represents one phase of research carried out at the Jet Propulsion Laboratory, California Institute of Technology, under NASA Contract NAS7-100. The author would like to thank Dr. E. Tward for his valuable suggestions and Mrs. G. McKay for her preparation of the manuscript.

QUESTIONS

Dr. H. P. Lee, NASA/GSFC

1. In your computer program, did you use empirical expressions or analytical relations for the charcoal adsorption coefficients for different media? If so, are they available?
2. How did you enter the temperature dependent thermophysical properties, such as thermal capacity, in your computation (based on what temperature to start)?

Dr. Al Sherman, NASA/GSFC

1. Have you run any system transient analyses for a space environment?

Author's Comments to Dr. Lee:

The adsorption coefficient used in the computer code was obtained from the generalized equation (eq. 3) which in turn was derived from the experimental data of References 6, 7 and 8. These references are available in the open literature.

The temperature-dependent thermophysical properties were incorporated in the computation process by averaging out the properties over the temperature swing of the complete cycle, (Reference 11).

Author's Comments to Dr. Sherman:

We have developed another program to analyze the transient behavior of the compressor. The results will be presented at the 1983 Cryogenic Engineering Conference in Colorado Springs.

Table 1. Gas Properties and Constants for Gas Conductivities and Isotherms Correlations

Gas	Helium	Hydrogen	Neon	Nitrogen
Molecular Weight (gm/g mole)	4.003	2.016	20.183	28.016
Inversion Temperature ($^{\circ}$ K)	40	202	250	622
Critical Point Pressure, P_{cr} (ATM)	2.26	12.8	26.9	33.5
Temperature, T_{cr} ($^{\circ}$ K)	5.2	33.3	44.5	126.2
Specific Volume, V_{cr} (cm^3/g)	14.4	32.2	2.067	3.21
Fusion Temperature K	2.17	13.9	24.57	63.
Van der Waal's Volume b ($\text{cm}^3/\text{g mole}$)	24	26.08	17	38.6
Parachor, β Cal/g mole	20.4	34.2	25.0	60.0
Constants for Thermal Conductivity Correlations				
a	0.7378	0.985	--	--
c	1.3258×10^7	7.81154×10^5	--	--
For Temperature Range	20K < T < 300K			
Constants for Isotherm Correlations Kidnay & Hiza [8]				
a	0.6722	0.40401	0.2961	0.40401
γ	0.0929	0.02870	0.0509	0.02870
	$13 < x < 30$	$0 < x < 25$	$0 < x < 20$	$0 < x < 25$
Tward et al [7]				
a	--	0.7875	0.304	--
γ	--	0.06466	0.0679	--
		$12 < x < 50$	$10 < x < 50$	

Table 2. Physical Properties of Charcoal, Stainless Steel and Copper

	Charcoal	Stainless Steel	Copper
Density, ρ gm/cc	0.466	7.82	8.94
Heat Capacity, C_p J/g - deg K			
20 $^{\circ}$ K	6.3×10^{-3}	4.6×10^{-3}	7.7×10^{-3}
80 $^{\circ}$ K	9.7×10^{-2}	1.6×10^{-1}	2.05×10^{-1}
100 $^{\circ}$ K	1.40×10^{-1}	2.4×10^{-1}	2.54×10^{-1}
200 $^{\circ}$ K	4.14×10^{-1}	4.1×10^{-1}	3.56×10^{-1}
300 $^{\circ}$ K	7.16×10^{-1}	4.8×10^{-1}	3.86×10^{-1}
400 $^{\circ}$ K	1.089		
500 $^{\circ}$ K	1.215		
Average Value J/g - deg K			
20-80K	0.045	0.0725	--
80-140K	0.166	0.267	--
140-200K	0.326	0.385	--
200-260K	0.505	0.448	--
260-300K	0.655	0.448	--
300-500K	1.03	0.532	--
Yield Strength, σ_y atm			
20K	--	4100	--
80K	--	3900	--
200K	--	2925	--
300K	--	2721	--

Table 3: Minimum Values of Specific Power, Compressor Mass For Unit Refrigeration Load and Cycle Time at Operating High Compressor Pressure P_H and Temperature T_3 for specified Precool Temperature T_P , Low Compressor Pressure P_L , and Temperature T_1

Gas	P_L atm	T_P K	T_1 K	T_3 K	P_H atm	Min Specific Power	m/Q_r g/W	t_o sec
Helium	0.68	25.5	26.6	67	20	20.	8.07	1.49
	1.00	25.5	26.5	67	20	17.7	6.91	1.49
	1.00	20	21	51	20	6.49	4.01	11.2
Neon	1.0	77	78	238	60	101.	6.54	7
	3.0	77	78	198	50	61.8	5.27	6.03
	5.0	77	78	178	40	49.7	4.87	5.2
Hydrogen	1.0	77	78	218	40	66.6	4.41	5.67
	3.0	77	78	198	40	41.3	3.31	5.45
	5.0	77	78	178	40	33.5	3.34	5.20
Nitrogen	1.0	150	151	501	70	104	1.92	9.64
	3.0	150	151	501	70	70.4	1.30	9.64
	5.0	150	151	471	70	60.7	1.26	9.34
	1.0	133	134	474	60	54.2	1.03	9.07
	3.0	133	134	474	70	39.1	0.92	9.45
	5.0	133	134	454	70	34.1	0.749	9.27

Table 4: Power, Cycle Time and System Mass for Helium, Hydrogen and Nitrogen Gas Adsorption Systems

Gas Adsorption System	Helium	Hydrogen	Nitrogen
Refrigeration Temperature, K	4	20	77
Precool Temperature, K	20	77	133
Compressor Operating Conditions			
P_L , atm	1.0	1.0	1.0
P_H , atm	20.0	40.0	60.0
T_1 , K	21.0	78.0	134.0
T_3 , K	51.0	218.0	474.0
Heat required (W) Per Unit Watt of Refrigeration Load	6.5	66.6	54.2
Cycle Time(s)*	110	56.7	90.7
Mass of Two (2) Compressors* (gm) Per Unit Watt of Refrigeration Load	80.02	88.2	20.3
Mass of J-T Valve and Counter Flow Heat Exchanger (gm/W)	227.4	4.31	2.54
System Mass (gm) per Watt of Refrigeration Load	307.42	92.51	32.84

* Based on $\delta = 0.1$ cm

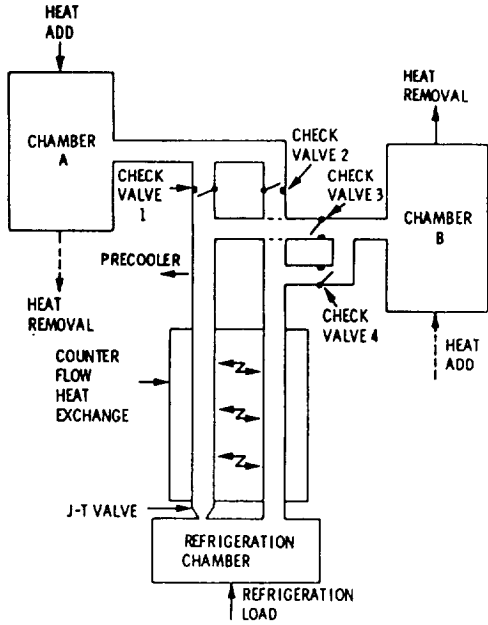


Fig. 1. Gas Adsorption Refrigeration System

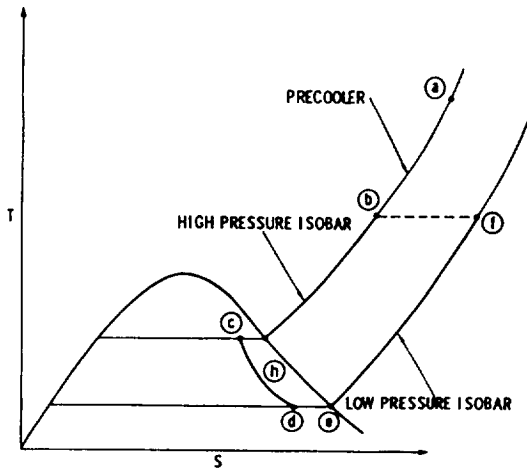


Fig. 3. Thermodynamical diagram of J-T Cooling

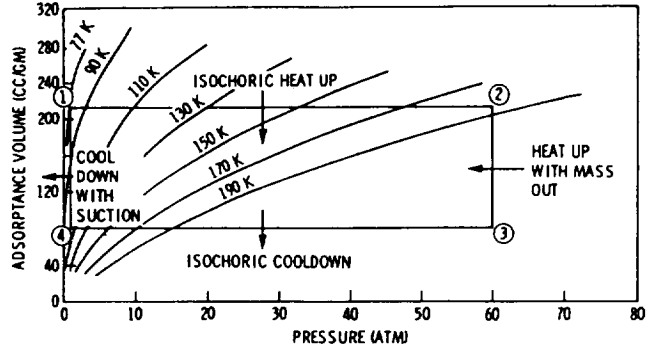


Fig. 2. Thermodynamical Cycle of Gas Adsorption and Desorption Processes for H_2

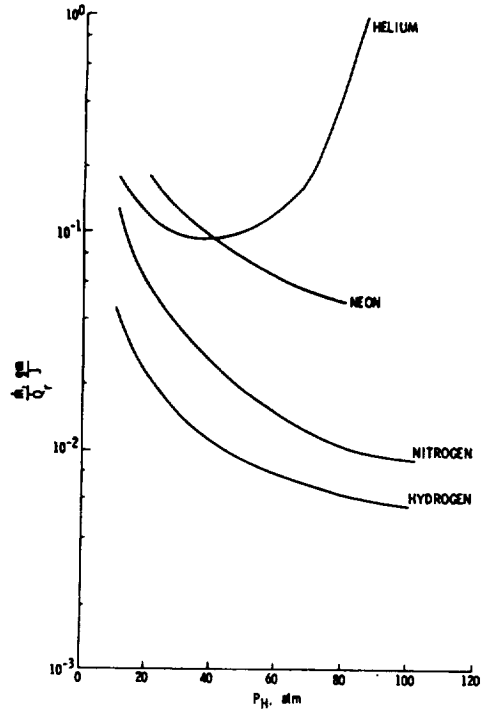


Fig. 4. Mass Flowrate for a Unit of Refrigeration Load for Four Different Gases

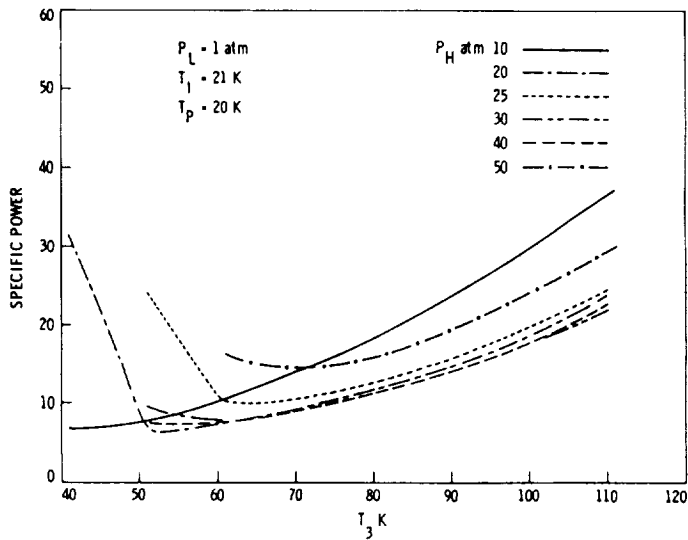


Fig. 5. Specific Power vs Maximum Compressor Temperatures for Various Nitrogen Compressor Pressures

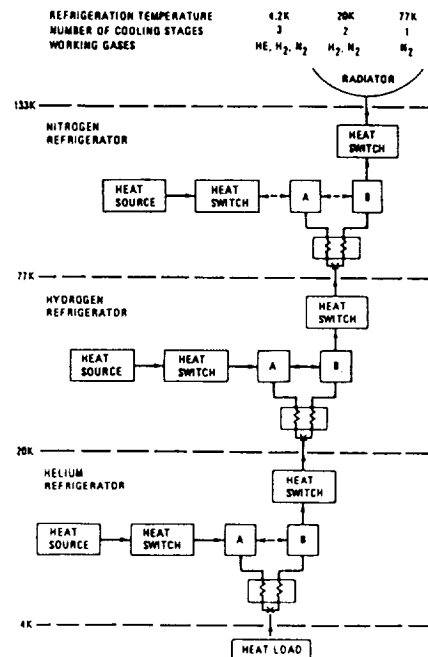


Fig. 6. Multistage Refrigerator Designs for Refrigeration Temperatures Varying from 4.2K to 77K.

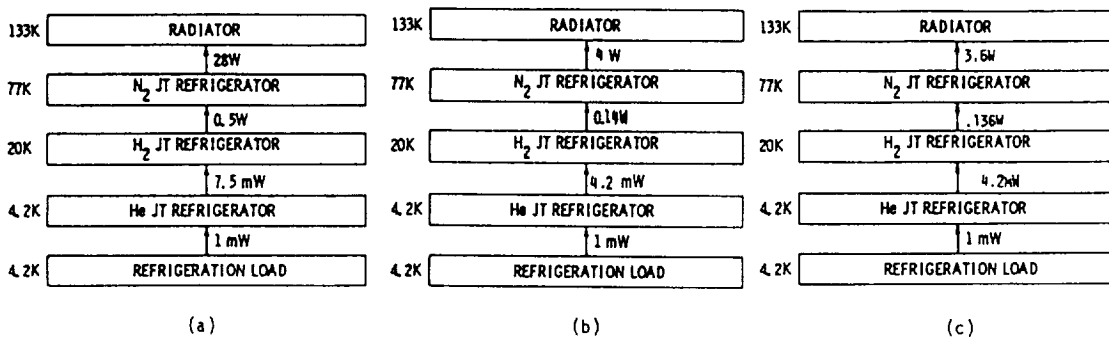


Fig. 7. Comparisons of Three Multi-stage Gas Adsorption Refrigerator Systems Performance for

- (a) with no heat recovery (b) with internal heat recovery (c) with internal and external heat recovery

REFERENCES

1. Chan, C. K.: Cryogenic Refrigeration Using a Low Temperature Heat Source, *Cryogenics*, vol. 21, 1981, pp. 291-399.
2. Elleman, D. D.; Petrac, D.; Chan, C. K.; and Tward, E.: Thermal Stability and Noise of a Miniature J-T Heat Exchanger Refrigerator System, *Proceedings of the 9th International Cryogenic Engineering Conf.*, (1982) p. 385.
3. Chan, C. K.; Tward, E.; and Elleman, D. D.: Miniature J-T Refrigerators Using Adsorption Compressors. *Advances in Cryogenic Engineering*, vol. 27, 1981, pp. 735-743.
4. Tward, E.: Gas Heat Switches. *Refrigeration for Cryogenic Sensors and Electronic Systems*, NBS Special Publication 607, 1981, pp. 178-185.
5. Kidnay, A. J.; and Hiza, M. J.: Physical Adsorption in Cryogenic Engineering. *Cryogenics*, vol. 10, 1970, pp. 271-276.
6. Yang, L. C.; Vo, T. D.; and Buriss, H. H.: Nitrogen Adsorption Isotherms in Zeolite and Activated Carbon, vol. 22, 1982, pp. 625-634.
7. Tward, E.; Marcus, C.; Chan, C. K.; Gatewood, J.; Steyert, W. A.; and Elleman, D. D.: High Pressure Adsorption Isotherms of H₂ and Neon on Charcoal, *Proceedings of the 9th International Cryogenic Engineering Conf.*, (1982) p. 34.
8. Kidnay, A. J.; and Hiza, M. J.: High Pressure Adsorption Isotherms of Neon, Hydrogen and Helium at 76°K. *Advances in Cryogenic Engineering*, vol. 12, 1966, pp. 730-740.
9. Cook, W. H.; and Basmadjian, D.: Correlation of Adsorption Equilibria of Pure Gases on Activated Carbon. *Canadian J. of Chem. Eng.*, vol. 42, 1964, p. 146.
10. Tward, E.: (private communication)
11. Chan, C. K.; Tward, E.; Elleman, D. D.: Kinetics of Gas Adsorption Compressor, Accepted for oral presentation at Cryogenic Engineering Conference, August 15-19, 1983, Colorado Springs, CO.